relative to the dication, by anionic detergent.[12] From the ESR and electronic spectra, this would correspond to the species A615. Loss of the remaining proton and Ph_3P ligand(s) produces CuTPP. If the proton and Ph_3P are not lost in a concerted fashion, then it seems likely that proton loss would be the first of a two-step process. This would produce a neutral "incipient" CuTPP species. The species F464 appears to be a neutral metalloporphyrin in which the copper is out of plane. This would thus correspond to CuTPP, in which the copper is out of plane and still contains at least one coordinated Ph_3P ligand or any solvent molecules or detergent anions which may be associated with the copper or the complex itself. (See Scheme I.)

Although we have no conclusive evidence for the exact nature of the proposed species, we do feel that they are chemically reasonable and consistent with the experimental data. If correct, they provide considerable insight into the details of a mechanism of metal ion incorporation by porphyrins at water–oil interfaces.

Acknowledgment. The authors wish to thank Mr. M. Del Vacchio and particularly Mr. C. Jones for their technical assistance. Special thanks are due to Dr. F. R. Longo for many helpful discussions.

Registry No. Copper, 7440-50-8; tetraphenylporphine, 917-23-7; benzene, 71-43-2; cyclohexanol, 108-93-0; sodium cetyl sulfate, 1120-01-0; triphenylphosphine, 603-35-0; CuTPP, 14172-91-9.

References and Notes

(1) K. Letts and R. A. Mackay, *Inorg. Chem.*, preceding paper in this issue.
(2) P. Hambright, *Coord. Chem. Rev.*, **6**, 247 (1971).
(3) E. B. Fleischer and J. H. Wang, *J. Am. Chem. Soc.*, **82**, 3498 (1960).
(4) E. B. Fleischer, E. J. Choi, P. Hambright, and A. Stone, *Inorg. Chem.*, **3**, 1284 (1964).
(5) P. Hambright, *J. Inorg. Nucl. Chem.*, **32**, 3449 (1970).
(6) S. J. Baum and R. A. Plane, *J. Am. Chem. Soc.*, **88**, 910 (1966).
(7) B. F. Burnham and J. J. Zuckerman, *J. Am. Chem. Soc.*, **92**, 1547 (1970).
(8) H. Baker, P. Hambright, and L. Wagner, *J. Am. Chem. Soc.*, **95**, 5942 (1973).
(9) E. B. Fleischer and F. Dixon, paper presented at 166th National Meeting of the American Chemical Society, Chicago, Ill., 1973.
(10) R. Nakamoto and P. J. McCarty, "Spectroscopy and Structure of Metal Chelate Compounds", Wiley, New York, N.Y., 1968, p 238.
(11) G. D. Dorough, J. R. Miller, and F. M. Huennekens, *J. Am. Chem. Soc.*, **73**, 4315 (1951).
(12) J. E. Falk, "Porphyrins and Metalloporphyrins", Elseveir, Amsterdam, 1964, pp 27–29; J. N. Phillips, *Curr. Trends Heterocycl. Chem., Proc. Symp.*, 30–37 (1958).

Contribution from the Lash Miller Chemical Laboratories, University of Toronto, Toronto, Ontario, Canada

Dissymmetric Arsine Complexes. An Interpretation of the d–d Electronic Absorption Spectra of Five-Coordinate Nickel(II), Palladium(II), and Platinum(II) Complexes and Their Axial-Group Interchange and Exchange Mechanisms

B. BOSNICH,* W. G. JACKSON, and S. T. D. LO

Received April 17, 1975 AIC50271C

A series of five-coordinate complexes of the type $[M(tetars)X]^+$, where tetars is a linear quadridentate tetra(tertiary arsine) ligand, where M = Ni(II), Pd(II), or Pt(II) and where X is a halide ligand, have been prepared and characterized. The absorption and circular dichroism spectra of these square-pyramidal complexes show consistent patterns and suggest that the d-orbital functions have the ordering $d_{xy} < d_{xz}, d_{yz} < d_{z^2} << d_{x^2-y^2}$. The halogeno ligands, although very stable in nonpolar solvents, are at the same time very labile at 30°. A variable-temperature NMR study indicates that both axial-site interchange and intermolecular exchange can occur by three different bimolecular mechanisms which involve halogen attack of the metal, as well as attack by either a four- or a five-coordinate complex resulting in the formation of dimers.

The diamagnetic five-coordinate complexes of Ni(II), Pd(II), and Pt(II) containing soft donor atoms such as arsenic and/or phosphorus have been the subject of continuing interest since the early work of Nyholm,[1-3] who isolated and characterized derivatives of the type $[M(diars)_2X]ClO_4$. All of these species are square-pyramidal complexes and it was only later that Venanzi[4-6] showed that, with appropriately designed ligands, diamagnetic trigonal-bipyramidal complexes of Ni(II) were equally accessible and were apparently of similar stability. In addition, Venanzi characterized the d–d spectra of the latter and showed them to be diagnostic of the geometry.

We recently described the preparation of a series of Co(III) complexes containing the quadridentate ligand tetars[7,8] and showed how the isomers of the ligand could be separated and resolved by means of their metal complexes. The *ms*-tetars ligand was shown to prefer a trans arrangement of its four arsenic atoms but the racemic ligand was flexible in its topological proclivities, giving cis-α, cis-β, and trans isomers in varying proportions depending upon the nature of the other coordinating ligands.[8] It was therefore of interest to see if this topological flexibility would extend to the d^8 systems, particularly those of divalent nickel, where the square-pyramidal and trigonal-bipyramidal stereochemistries might be of similar energies. We will show, however, that this is not the case for these ligands; all contain a planar array of arsenic donor atoms in a large variety of solvents. Besides this stereochemical aspect, only one report[9] of a systematic interpretive study of the electronic spectra of square-pyramidal systems has appeared. The assignments in this recent study[9] were based on the temperature-dependent profiles of the d–d bands and their energy displacements upon axial substitution. In the present work we amplify, and essentially confirm, the assignments of the previous study by an analysis of the circular dichroism spectra, which provide a precise probe into the magnetic dipole character of the transitions and are capable of resolving features which are hidden beneath the broad manifolds observed in the normal linear absorption. The final aspect of interest is that the fifth coordinated ligand, X, which is usually a halogen or pseudohalogen, is very stable,[10] although chemical evidence suggests that, at the same time, it is very labile in solution at room temperature. The $[Ni(diars)_2X]^+$ ions, although having some of the convenient simplicity in their

Table I. Conductance[a] (Λ_M) for Ni(II) Complexes

Compd	CH_2Cl_2	$(CH_3)_2CO$	CH_3CN	CH_3OH
[Ni(*R*,*R*:*S*,*S*-tetars)CH_3CN]$(ClO_4)_2$			260 (2:1)	
[Ni(*R*,*S*-tetars)CH_3CN]$(ClO_4)_2$			254 (2:1)	
[Ni(*R*,*R*:*S*,*S*-tetars)]$(ClO_4)_2$	10 (1:1)	128 (1:1)		118 (1:1)[b]
[Ni(*R*,*S*-tetars)]$(ClO_4)_2$	17 (1:1)	121 (1:1)		103 (1:1)[b]
[Ni(*R*,*R*:*S*,*S*-tetars)Cl]ClO_4	32 (1:1)	125 (1:1)	120 (1:1)	81 (1:1)
[Ni(*R*,*S*-tetars)Cl]ClO_4	37 (1:1)	125 (1:1)	120 (1:1)	84 (1:1)
[Ni(*R*,*R*:*S*,*S*-tetars)Br]ClO_4	33 (1:1)	128 (1:1)	130 (1:1)	78 (1:1)
[Ni(*R*,*S*-tetars)Br]ClO_4	38 (1:1)	126 (1:1)	123 (1:1)	83 (1:1)
[Ni(*R*,*R*:*S*,*S*-tetars)I]ClO_4	31 (1:1)	117 (1:1)	128 (1:1)	78 (1:1)
[Ni(*R*,*R*:*S*,*S*-tetars)I]I	41 (1:1)	128 (1:1)	132 (1:1)	87 (1:1)
[Ni(*R*,*S*-tetars)I]ClO_4	35 (1:1)	125 (1:1)	117 (1:1)	80 (1:1)

[a] All conductances refer to 10^{-3} *M* solutions at 25°. [b] The visible absorption spectra are concentration dependent in the range 5×10^{-3} to 5×10^{-4} *M*; all of the other spectra are concentration independent in this range.

Table II. Conductance[a] (Λ_M) for Pd(II) Complexes

Compd	CH_2Cl_2	CH_3CN	CH_3OH	H_2O
[Pd(*R*,*R*:*S*,*S*-tetars)]$(ClO_4)_2$		255 (2:1)[b]		
[Pd(*R*,*S*-tetars)]$(ClO_4)_2$	12 (1:1)	210 (2:1)[b]	87 (1:1)[b]	
[Pd(*R*,*R*:*S*,*S*-tetars)Cl]Cl	21 (1:1)	124 (1:1)[b]	96 (1:1)[b]	189 (2:1)
[Pd(*R*,*S*-tetars)Cl]Cl	26 (1:1)	113 (1:1)[b]	68 (1:1)[b]	175 (2:1)
[Pd(*R*,*R*:*S*,*S*-tetars)Cl]ClO_4	21 (1:1)	143 (1:1)[b]		
[Pd(*R*,*S*-tetars)Cl]ClO_4	28 (1:1)	129 (1:1)[b]	79 (1:1)[b]	
[Pd(*R*,*R*:*S*,*S*-tetars)Br]ClO_4	21 (1:1)	151 (1:1)[b]		
[Pd(*R*,*S*-tetars)Br]ClO_4	25 (1:1)	142 (1:1)[b]	86 (1:1)[b]	
[Pd(*R*,*R*-tetars)I]I	19 (1:1)	105 (1:1)[b]	71 (1:1)[b]	
[Pd(*R*,*S*-tetars)I]I	29 (1:1)	120 (1:1)[b]	75 (1:1)[b]	

[a] Conductances are for 10^{-3} *M* solutions at 25°. [b] The near-ultraviolet spectra are concentration dependent in the range 5×10^{-3} to 5×10^{-4} *M*; all other spectra are concentration independent in this range. (The d–d spectra are not resolved in the diperchlorate complexes.)

NMR spectra to study the lability of the X group, are not sufficiently soluble at low temperatures in common acceptable solvents. The corresponding tetars systems are more soluble and in addition possess the required stereochemical subtlety to elicit the mechanisms of X group exchange.

This paper describes the preparation and properties of the tetars complexes of Ni(II), Pd(II), and Pt(II), an interpretation of their d–d electronic spectra, and a study of the lability of the X groups in the complexes of the type [M(tetars)X]ClO_4. The two (stable) isomers of the tetars ligand are shown in Figure 1.

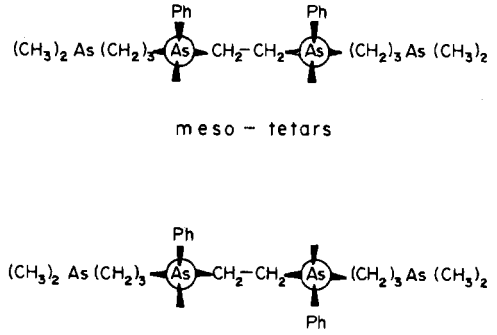

Figure 1. Structures of the two arsines.

1. Preparations and Properties

The diperchlorate salts of the *rac*-tetars, active tetars, and *ms*-tetars complexes of Ni(II) are simply prepared by allowing stoichiometric amounts of the appropriate arsine in ether to react with $[Ni(H_2O)_6](ClO_4)_2$ in acetone. The five-coordinate species $[Ni(tetars)X]^+$ (where $X^- = Cl^-$, Br^-, or I^- for active tetars and *ms*-tetars and where $X^- = Cl^-$, Br^-, I^-, or NCS^- for the racemic tetars) are generated by adding the appropriate halide ion to the [Ni(tetars)]$(ClO_4)_2$ complexes in any of the solvents CH_3CN, CH_3OH, or acetone. In all cases the equilibrium lies essentially toward the $[Ni(tetars)X]^+$ species. The isolation of these complexes as either the ClO_4^- or the corresponding X^- salts, however, depends critically on the conditions used for crystallization; the less soluble salt is always produced. For example, [Ni(*R*,*R*:*S*,*S*-tetars)I]ClO_4 and [Ni(*R*,*S*-tetars)I]ClO_4 can be isolated from acetone only provided no more than a 1:1 equivalent of NaI is present and an excess of $LiClO_4$ is used. No method was found which gave the [Ni(*R*,*R*-tetars)I]ClO_4 salt pure; it was isolated as the iodide.

The five-coordinate halogeno complexes are 1:1 electrolytes in methanol, methylene chloride, acetone, and also acetonitrile, and, furthermore, their visible absorption spectra in these solvents are concentration independent in the range 1×10^{-3} to 5×10^{-4} *M*. The diperchlorate salts are also 1:1 electrolytes in methylene chloride and acetone, and their spectra in these solvents are concentration (1×10^{-3} to 5×10^{-4} *M*) independent. In methanol, however, 10^{-3} *M* solutions have conductances somewhat higher than 1:1 electrolytes and their visible spectra are concentration dependent. If an excess of $LiClO_4$ is added, a limiting spectrum is obtained for both the *rac*- and *ms*-tetars diperchlorate complexes. This suggests that both the complexes exist at these concentrations, $\sim 10^{-3}$ *M*, as perchlorate-associated species in equilibrium in methanol solutions. The diperchlorate–nickel(II) complexes of both of the tetars ligands display, in acetonitrile, spectra which are distinctly different from those observed in the other solvents and behave as 2:1 electrolytes. The deep brown complexes can be isolated and both analyze for the formula [Ni(tetars)CH_3CN]$(ClO_4)_2$. When these solids are dissolved in either acetone, methylene chloride, or methanol, the coordinated acetonitrile molecule is lost upon dissolution. Free acetonitrile is detected in the NMR spectra, and the visible absorption spectra correspond to those found for the perchlorate salts. The conductivity data[11] are summarized in Table I.

Perhaps, suprisingly, the five-coordinate tetars complexes of palladium appear to be less stable with respect to dissociation of the fifth ligand than the corresponding Ni(II) complexes (Table II). The Pd(II) complexes were prepared by allowing the tetars ligands to react with $[Pd(CH_3CN)_2Cl_2]$ to give the [Pd(tetars)Cl]Cl complexes in high yield. The

Table III. Conductance[a] (Λ_M) for Pt(II) Complexes

Compd	CH_2Cl_2	CH_3CN	CH_3OH
[Pt(*R*,*R*:*S*,*S*-tetars)]$(ClO_4)_2$		270 (2:1)[b]	
[Pt(*R*,*S*-tetars)]$(ClO_4)_2$	13 (1:1)[b]	222 (2:1)[b]	
[Pt(*R*,*R*:*S*,*S*-tetars)I]I	19 (1:1)	105 (1:1)[b]	71 (1:1)
[Pt(*R*,*S*-tetars)I]I	29 (1:1)[b]	112 (1:1)[b]	74 (1:1)

[a] Conductances for 10^{-3} *M* solutions at 25°. [b] The near-ultraviolet spectra are concentration dependent in the range 5×10^{-3} to 5×10^{-4} *M*. (The diperchlorate complexes show no resolved d–d spectra.)

solubility relationships between the various salts were such, however, that not all of the [Pd(tetars)X]ClO_4 compounds could be obtained. The various complexes isolated are listed in Table II together with their conductivities and the concentration dependence of their near-ultraviolet spectra. It is only in the weakly solvating methylene chloride solutions that the complexes are five-coordinate—even [Pd(*R*,*S*-tetars)ClO_4]ClO_4 is a 1:1 electrolyte. Unlike the nickel complexes, in acetonitrile and methanol all of the complexes show concentration-dependent spectra. In water the two [Pd(tetars)Cl]Cl complexes are fully dissociated.

The five-coordinate Pt(II) complexes proved to be the most difficult to isolate, although the addition of halide ions to weakly polar solutions of the diperchlorates resulted in the production of the characteristic brightly colored solutions. We have only isolated the two pairs of species listed in Table III. The concentration dependence of the spectra may indicate ion-pair formation or a tendency to six-coordination depending on the structure of the ion pair.

Thus the successful isolation of these stable but kinetically labile five-coordinate complexes depends on the solvation energies of the various ions and the solubility products of the possible complex salts.

2. Electronic Spectra

The structures of these complexes cannot be established by NMR spectra at room temperature for reasons which we shall discuss presently. In solvents where the complexes are five-coordinate, the spectra, both linear and circular dichroism of any particular complex, show only small variations. If the species exist as mixtures of isomers where the ligands are arranged in cis-α, cis-β, or trans topologies, we would expect the concentrations of the species to change from solvent to solvent, as was observed for the Co(III) complexes.[7,8] Such equilibrium changes would be seen in their spectra since the absorption intensities and positions are expected to be very sensitive to the isomerism. Furthermore, the d–d absorption bands of these complexes are very similar, in both position and intensity, to those of the corresponding members of the $[M(diars)_2X]^+$ series[1-3] which are square pyramidal with axial X groups. Finally, circular dichroism intensities associated with the d–d bands of these species are about the same as are observed for the *trans*-[Co(*R*,*R*-tetars)(H)X]$^+$ ions,[12] the d–d transitions of which have similar transition magnetic dipole moments. Thus both the absorption and circular dichroism spectra indicate that all of the present series of complexes are square pyramidal with four planar arsenic atoms.

a. Ni(II) Complexes. We classify the metal d-orbital functions of the central metal atoms of these molecules according to the C_{4v} point group. The spin-allowed d–d transitions are, therefore, $^1A_1 \rightarrow {}^1B_1$ ($d_{z^2} \rightarrow d_{x^2-y^2}$), $^1A_1 \rightarrow {}^1E$ (d_{xz}, $d_{yz} \rightarrow d_{x^2-y^2}$), and $^1A_1 \rightarrow {}^1A_2$ ($d_{xy} \rightarrow d_{x^2-y^2}$) (Figure 2). Of these, the $^1A_1 \rightarrow {}^1E$ transition is both electric and magnetic dipole allowed, while the other two are forbidden in electric dipole radiation fields but $^1A_1 \rightarrow {}^1A_2$ is magnetic dipole allowed and $^1A_1 \rightarrow {}^1B_1$ is quadrupole allowed. These selection rules predict that the $^1A_1 \rightarrow {}^1E$ excitation should be the most intense while the $^1A_1 \rightarrow {}^1E$ and $^1A_1 \rightarrow {}^1A_2$ transitions should carry the stronger circular dichroism.[13] In addition to these criteria for assignment, there are the expected band shifts resulting from substitution at the axial positions. The $d_{x^2-y^2}$ and d_{xy} orbitals will experience essentially a constant ligand field, due to the planar array of arsenic atoms, as the axial

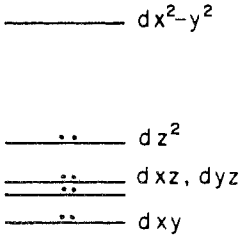

Figure 2. Ordering of the d-orbital states for the square-pyramidal complexes. Apart from configuration interaction, the $d_{z^2} \rightarrow d_{x^2-y^2}$ promotion should give an indication of the σ-bonding capacity of the axial ligand, and the d_{xz}, $d_{yz} \rightarrow d_{x^2-y^2}$ transition should reflect the π-bonding capacity of the axial ligand, while the remaining transition should be insensitive to axial perturbation.

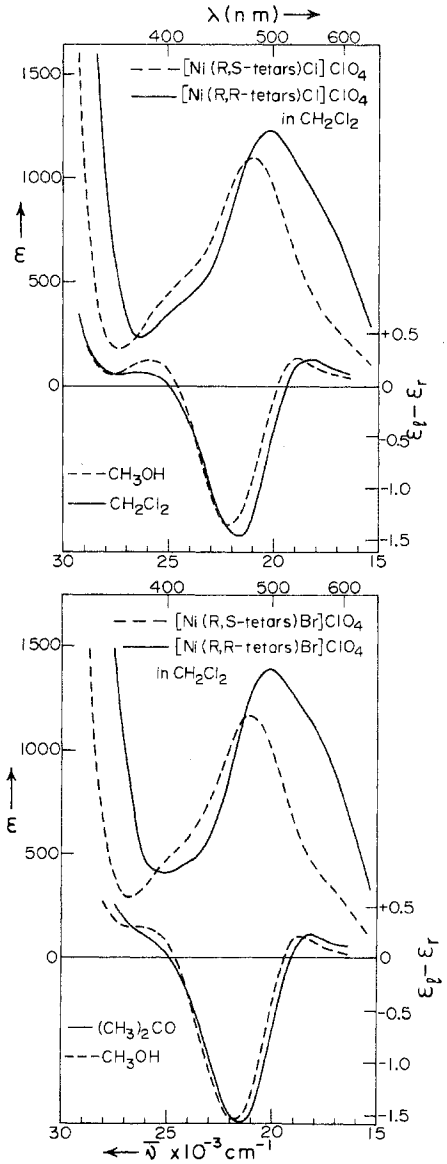

Figure 3. Absorption and circular dichroism spectra of the [Ni(tetars)X]ClO_4 (X = Cl, Br) complexes. Spectra for all of the compounds were measured in CH_2Cl_2, $(CH_3)_2CO$, CH_3OH, and CH_3CN. The variations in the absorption spectra are slight as are the variations in the circular dichroism spectra; in the latter the two spectra which show the maximum variation are drawn.

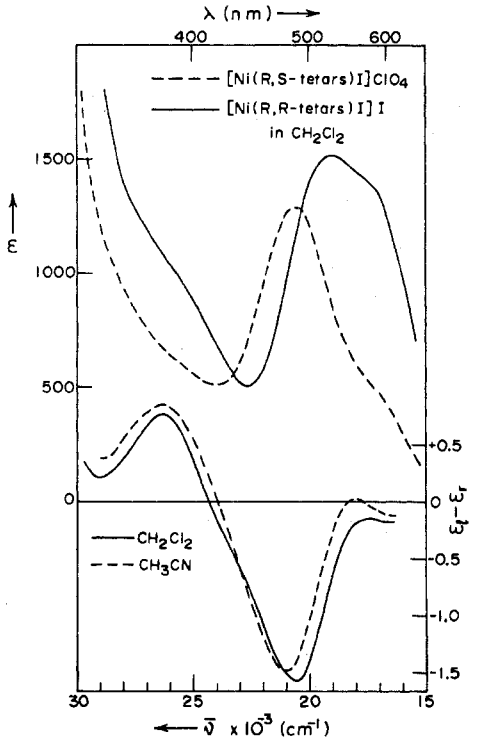

Figure 4. Absorption and circular dichroism spectra of the $[Ni(tetars)I]^+$ ions.

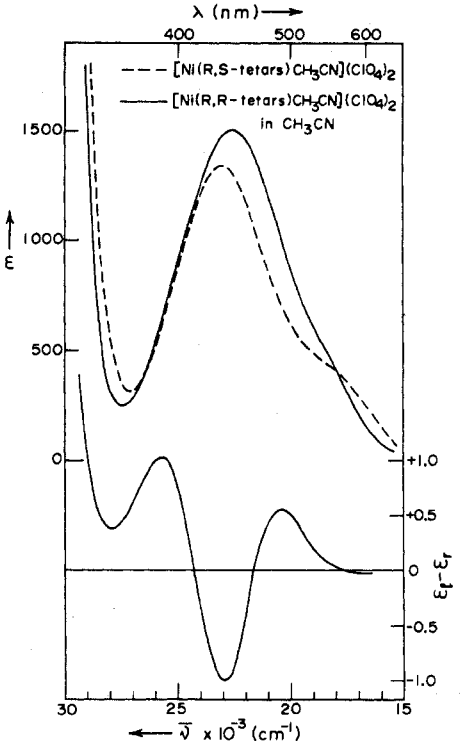

Figure 5. Absorption and circular dichroism spectra of the $[Ni(tetars)CH_3CN]ClO_4$ complexes.

group is varied. The $d_{z^2} \rightarrow d_{x^2-y^2}$ promotion, however, will be sensitive to the σ ligand field of the axial ligand while the d_{xz}, $d_{yz} \rightarrow d_{x^2-y^2}$ transition will be sensitive to the π-bonding of the axial group.

Figures 3 and 4 show the absorption and circular dichroism spectra of the $[Ni(R,R\text{-tetars})X]^+$ ions, $X^- = Cl^-$, Br^-, or I^-, and the absorption spectra of the $[Ni(R,S\text{-tetars})X]^+$ analogues. It is interesting that the corresponding absorption spectra of the racemic arsine complexes appear at lower energies than those of the meso arsine complexes. The higher ligand field of the meso ligand may be due to the different conformational demands of this ligand, which may give rise to shorter Ni–As bond lengths. All the absorption spectra are characterized by three d–d bands in the visible region: a low-energy weak-to-medium intensity transition, followed by a stronger intensity transition which dominates the spectra, and, finally, at 26,000 cm^{-1} a weak poorly resolved band. The position of this last band is insensitive to axial substitution, but the other two vary in energy as X is changed. We assign the 26,000-cm^{-1} band to the $^1A_1 \rightarrow {}^1A_2$ ($d_{xy} \rightarrow d_{x^2-y^2}$) excitation because of its insensitivity to axial substitution. The strong central band is assigned to the electric dipole allowed transition $^1A_1 \rightarrow {}^1E$ (d_{xz}, $d_{yz} \rightarrow d_{x^2-y^2}$) because of its intensity. The low-energy band is therefore assigned to the $^1A_1 \rightarrow {}^1B_1$ ($d_{z^2} \rightarrow d_{x^2-y^2}$) excitation, which, as expected, is weaker in intensity. The absorption maxima of the $^1A_1 \rightarrow {}^1B_1$ bands for these three complexes cannot be accurately determined, but the $^1A_1 \rightarrow {}^1E$ band follows the energy order $Cl^- > Br^- > I^-$ and suggests that the electrons of the filled π orbitals of the halogens destabilize the filled d_{xz}, d_{yz} levels in the order $I^- > Br^- > Cl^-$ (Figure 2).

Figures 5 and 6 show the spectra of the $[Ni(tetars)CH_3CN](ClO_4)_2$ and $[Ni(tetars)](ClO_4)_2$ complexes. For the acetonitrile adduct the strong band shifts to higher energies and obscures the $^1A_1 \rightarrow {}^1A_2$ transition; the lower energy band, $^1A_1 \rightarrow {}^1B_1$, however, remains in about the same position as for the halogeno complexes. This last observation suggests that the σ-donor capacity of the acetonitrile ligand is about the same as that of the halogen ligands. The π interactions

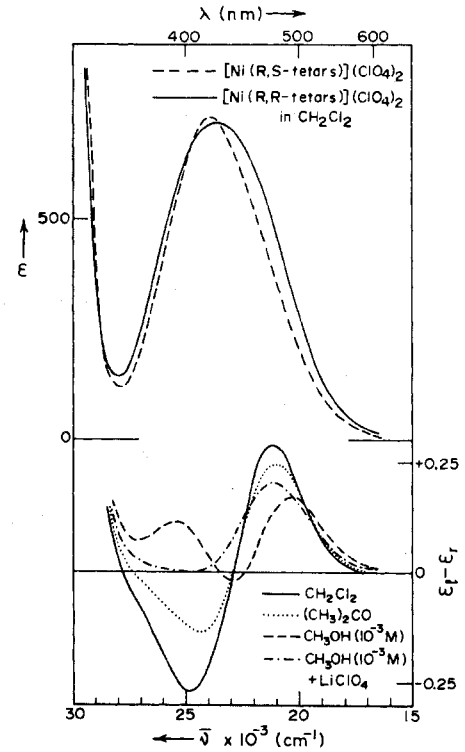

Figure 6. Absorption and circular dichroism spectra of the $[Ni(tetars)](ClO_4)_2$ complexes. The variations of the circular dichroism are shown; the curve represented as - · - · - is for a 10^{-4} *M* methanol solution of the complex saturated to incipient crystallization with $LiClO_4$. The absorption spectra in methanol show a decrease in intensity as $LiClO_4$ is added but the basic form of the spectrum remains the same.

of the filled π orbitals of the halogens with the filled d_{xz}, d_{yz} orbitals will be essentially destabilizing, and hence the origin of the higher energy shift of the $^1A_1 \rightarrow {}^1E$ band of the acetonitrile adduct is ambiguous. It could mean that there

is little or no (d–π)–(p–π) interaction between the empty acetonitrile π^* orbitals and the filled π orbitals of the metal or that any interaction is stabilizing. The $^1A \rightarrow {}^1E$ absorption maximum of the acetonitrile adduct and that of the perchlorato complex are at about the same energy (vide infra), which suggests that the π-stabilizing capacity of the acetonitrile adduct is small.

The conductivities of the perchlorate complexes in methylene chloride and acetone indicate that, at the concentrations used for obtaining the spectra, one of the ClO_4^- ions is associated to the complex. If this implies that the ClO_4^- ion is actually coordinated to the metal, its effect on the d-electron levels must be small, because the intensity of the absorption manifold is decreased by half, suggesting that the noncentric C_{4v} selection rules have been modified to rules which are better described by the centric D_{4h} point group. Furthermore, we expect the oxygen-donating ClO_4^- ligand to exert a ligand field which is about the same as that for other negatively charged oxygen donor ligands; this expectation is confirmed for the diamagnetic trigonal-bipyramidal complexes of nickel, which contain a coordinated perchlorato ligand.[4] Thus we conclude that the associated ClO_4^- ion in these complexes is not effectively coordinated to the metal.

The circular dichroism spectra of all the halogeno complexes were measured in methylene chloride, acetone, methanol, and acetonitrile. Each set of spectra are very similar, which supports our earlier suggestion that all have the same stereochemistry in all the media studied. When all the complexes are considered, the following interpretation of the circular dichroism spectra seems to us the most consistent, although for the halogeno complexes of nickel some of the assignments may initially appear arbitrary.

For the halogeno complexes we assign the positive circular dichroism bands at 26000 cm^{-1} to the $^1A_1 \rightarrow {}^1A_2$ transition, and the strong negative bands centered around 21000–22000 cm^{-1} to *one* of the components of the $^1A_1 \rightarrow {}^1E$ transition. It will be noted that this latter absorption is, in all cases, shifted to higher energies compared to the linear absorption maxima of the $^1A_1 \rightarrow {}^1E$ transition, as would be expected if the other component of the $^1A_1 \rightarrow {}^1E$ transition were positive and located slightly to lower energies. The circular dichroism in acetonitrile solutions below 20000 cm^{-1} for the iodo complex shows a very weak positive band at about 18000 cm^{-1} which is followed, to lower energies, by a negative band. In other solvents, this positive band does not emerge because of small solvent variations in the intensities of the overlapped contiguous circular dichroism bands of opposing sign. This is not an unusual phenomenon. We assign the positive band at 18000 cm^{-1}, seen in acetonitrile, to the other component of the $^1A_1 \rightarrow {}^1E$ transition and the negative band seen at lower energies to the $^1A_1 \rightarrow {}^1B_1$ transition. This latter band is not seen in the chloro and bromo complexes because of overlap with the positive lower energy component of the $^1A_1 \rightarrow {}^1E$ band. The spectra of the other complexes tend to support these assignments.

The acetonitrile adduct shows four circular dichroism bands which are assigned as follows. The very weak circular dichroism at 17000 cm^{-1} is assigned to the $^1A_1 \rightarrow {}^1B_1$ transition, the plus–minus couplet, centered at the absorption maximum of the $^1A_1 \rightarrow {}^1E$ band, is assigned to the components of this band, and the high-energy positive absorption around 26000 cm^{-1} is assigned to the $^1A_1 \rightarrow {}^1A_2$ transition, which is not resolved in the linear absorption spectrum. The perchlorate complex shows only a plus–minus couplet centered at the absorption maximum of the manifold of transitions and we assign it to the components of the $^1A_1 \rightarrow {}^1E$ transition. The $^1A_1 \rightarrow {}^1A_2$ band, which is positive in the other complexes and should occur at 26000 cm^{-1}, is probably effective in causing

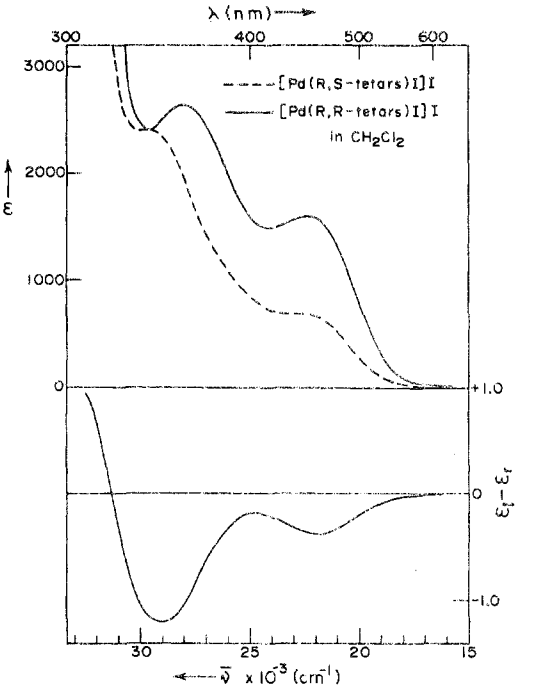

Figure 7. Absorption and circular dichroism spectra of the [Pd(tetars)I]I complexes.

the asymmetry at 26000 cm^{-1} in the negative band in solutions of methylene chloride and acetone. In methanol, where a limiting spectrum is obtained by adding $LiClO_4$, the negative component of the $^1A_1 \rightarrow {}^1E$ transition and the (positive) $^1A_1 \rightarrow {}^1A_2$ band nearly cancel. The weak $^1A_1 \rightarrow {}^1B_1$ band, which is expected to shift under the absorption manifold in this complex, is not observed.

All of these assignments are in conformity with the magnetic dipole selection rules[13] for optical activity, in that, the magnetic dipole allowed transitions, $^1A_1 \rightarrow {}^1A_2$ and $^1A_1 \rightarrow {}^1E$, show much stronger circular dichroism than the magnetic dipole forbidden $^1A_1 \rightarrow {}^1B_1$ transition.

b. Pd(II) Complexes. The palladium complexes show similar patterns, although only the iodo complex shows both the $^1A_1 \rightarrow {}^1E$ and $^1A_1 \rightarrow {}^1B_1$ bands (Figure 7) clearly resolved in the linear absorption. For the chloro and bromo complexes, the $^1A_1 \rightarrow {}^1E$ band is "lost" under the charge-transfer transitions, and only the $^1A_1 \rightarrow {}^1B_1$ transitions are seen in the linear absorption. For the iodo complex, the transition at 22000 cm^{-1} is assigned to the $^1A_1 \rightarrow {}^1B_1$ excitation, which carries negative circular dichroism, as it does in the nickel complexes. This band is also negative for the chloro and bromo complexes. For the racemic ligand complexes, this band in linear absorption occurs at 25000, 24000, and 22000 cm^{-1} for the chloro, bromo, and iodo complexes, respectively. Such an order suggests, perhaps surprisingly, that the σ-bonding capacities of the halogens to the d_{z^2} orbital follow the order $I^- > Br^- > Cl^-$. The ligand field strengths of ligands, of course, involve both the σ- and π-bonding capacities, and, in the present systems, the ligand field is measured by the difference in energy between the $^1A_1 \rightarrow {}^1E$ and $^1A_1 \rightarrow {}^1B_1$ transitions after configuration interaction is taken into account (Figure 2). It will be recalled that the π-destabilizing capacities of the halogens follow the order $I^- > Br^- > Cl^-$ for the nickel complexes.

Although $^1A_1 \rightarrow {}^1E$ is submerged under the charge-transfer bands in the chloro and bromo complexes, the circular dichroism shows a positive component to higher energies of the negative $^1A_1 \rightarrow {}^1B_1$ bands for both complexes and probably represents a component of the $^1A_1 \rightarrow {}^1E$ transition. The iodo complex, however, shows a negative trough at 25000 cm^{-1}

(Figure 7) and then a strong negative band, the maximum absorption of which lies to the higher energy side of the linear absorption maximum of the $^1A_1 \rightarrow {}^1E$ band. In view of the presence of couplets for this band in the nickel complexes and the positive bands observed immediately after the $^1A_1 \rightarrow {}^1B_1$ transition for the chloro- and bromopalladium complexes, it is probable that the negative trough at 25000 cm^{-1} observed for the iodo complex represents the overlapped positive component of the $^1A_1 \rightarrow {}^1E$ transition.

When the chloro and bromo complexes are dissolved in water, the solutions are colorless. The first linear absorption band is an intense (ϵ 22000 at 35500 cm^{-1}) charge-transfer transition, presumably involving the arsenic and palladium levels. The position and intensity of this band is the same for aqueous solutions of the chloro, bromo, and diperchlorate complexes. The d–d bands are under this transition and their presence is indicated by the circular dichroism, which shows the same pattern as observed for the nickel analogue in methylene chloride solution; a positive band is observed at 28000 cm^{-1}, and then an overlapped negative band, at 30000 cm^{-1}. These we ascribe to the $^1A_1 \rightarrow {}^1E$ transitions.

c. Pt(II) Complexes. The d–d bands of the platinum complexes, being at higher energies than the palladium analogues, are heavily overlapped by the intense charge-transfer transitions. The iodo complex, however, does show a resolved linear absorption band, which for the racemic ligand is at 26250 cm^{-1} (ϵ 2580) and carries negative circular dichroism and which we ascribe to the $^1A_1 \rightarrow {}^1B_1$ transition.

We make three observations about these spectra. The first is that the circular dichroism spectra show consistent patterns, provided the individual spectroscopic components are identified and the problems arising from overlapped bands of varying signs, intensities, and energy spacings are recognized. The second is that the spectra of these square-pyramidal d^8 systems provide a useful experimental method of separating π and σ interactions. This was recognized by Gray[9] for square-pyramidal complexes and by Venanzi[14] and Meek[6] for trigonal-bipyramidal complexes. Finally, the spectroscopic assignments indicate that the bright solutions obtained when halide ions are added to nonpolar solutions of platinum and palladium complexes are caused by a shift in the $d_{z^2} \rightarrow d_{x^2-y^2}$ excitation and are not, in general, due to charge-transfer bands as is sometimes supposed.

3. NMR Spectra

In a previous paper we showed[7] that complexes of the type *trans*-[M(*R*,*S*-tetars)X_2]$^{n+}$ as well as each of the two isomers of *trans*-[M(*R*,*S*-tetars)XY]$^{n+}$ show only two methyl proton resonances of equal area. (The two isomers arise because, in the complexed meso ligand, both phenyl groups lie on one side of the As_4 plane.) The racemic ligand coordinated in the complexes of the type *trans*-[M(*R*,*R*:*S*,*S*-tetars)X_2]$^{n+}$ and *trans*-[M(*R*,*R*:*S*,*S*-tetars)XY]$^{n+}$ shows two and four methyl proton resonances, respectively. Therefore, we would expect the five-coordinate complexes [M(*R*,*R*:*S*,*S*-tetars)X]$^+$ to show four methyl proton resonances and, if both isomers exist, the *trans*-[M(*R*,*S*-tetars)X]$^+$ ions may also show four methyl proton resonances, two for each isomer.

a. Phenomena. These do not obtain at 30° for either (tetars) isomer dissolved in a variety of solvents; for both the racemic and meso five-coordinate complexes, only two sharp methyl proton resonances are observed. Moreover, if any pair of five-coordinate complexes of the racemic ligand, [Ni(*R*,*R*:*S*,*S*-tetars)X]ClO_4 and [Ni(*R*,*R*:*S*,*S*-tetars)X']ClO_4 (X $\neq$ X' = Cl, Br, I), is mixed, only two sharp methyl proton resonances are observed at 30°, the chemical shifts of which correspond to the concentration-weighted mean of the corresponding methyl proton signals of the individual species. Similarly, if any pair of complexes derived from the meso ligand, that is [Ni(*R*,*S*-tetars)X]ClO_4 and [Ni(*R*,*S*-tetars)X']ClO_4 where X $\neq$ X' = Cl, Br, I, is mixed at 30°, again only two sharp methyl proton resonances are observed, at the concentration-weighted mean of the corresponding resonances of the individual complexes. However, if the analogous meso and racemic complexes [Ni(*R*,*S*-tetars)X]ClO_4 and [Ni(*R*,*R*:*S*,*S*-tetars)X]ClO_4, where X = Cl, Br, or I, are mixed at 30°, four sharp methyl proton signals are observed, corresponding, exactly, to the chemical shifts observed for the individual separated species.

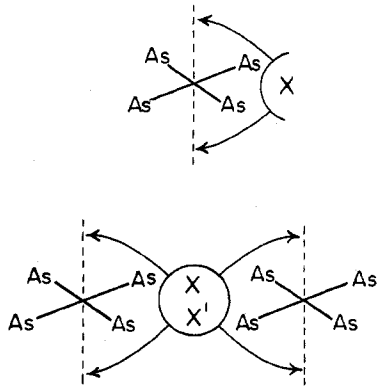

Figure 8. Top: Proposed axial interchange of the X group leading to magnetic equivalence. Bottom: proposed intermolecular exchange of the X and X' groups with the axial sites of two planar $[M(tetars)]^{2+}$ ions.

We interpret these observations as follows. Since at 30° the complexes [Ni(*R*,*R*:*S*,*S*-tetars)X]ClO_4 behave as if the two axial environments are equivalent, we assume that rapid axial-site interchange is occurring by the transference of the X ligand from one (equivalent) apical position to the other (Figure 8). The uncoordinated apical positions of the [Ni(*R*,*S*-tetars)X]ClO_4 complexes are not equivalent and hence the NMR results are equivocal; either one apical isomer exists or there is rapid apical-site interchange. When the pairs of complexes [Ni(*R*,*R*:*S*,*S*-tetars)X]ClO_4 and [Ni(*R*,*R*:*S*,*S*-tetars)X']ClO_4 are mixed, apical-site interchange proceeds at the individual species but, in addition, intermolecular exchange between X' and X occurs (Figure 8). The same intermolecular X' and X exchange occurs for the [Ni(*R*,*S*-tetars)X']ClO_4 and [Ni(*R*,*S*-tetars)X]ClO_4 mixtures irrespective of whether or not simultaneous axial-site exchange is occurring. And, finally, the NMR spectra of the [Ni(*R*,*R*:*S*,*S*-tetars)X]ClO_4 and [Ni(*R*,*S*-tetars)X]ClO_4 mixtures indicate that at 30° the *R*,*R*:*S*,*S*-tetars and *R*,*S*-tetars ligands are not exchanging on an NMR time scale.

We have attempted to elicit the mechanisms of these processes by a temperature-dependent study of the NMR spectra in methylene chloride but the conclusions are circumscribed by two factors. First, the methyl proton signals, although clearly resolved, lie above the broad manifold of signals associated with the ligand methylene protons which, in most cases, experience drastic chemical shifts and changes in resolution as the temperature is varied. This together with the electronic senility of our present spectrometer prevented a detailed analysis of the temperature variations. Second, for practical reasons, our conclusions refer to the restricted concentration range between 0.01 and 0.04 *M* for solutions of the individual complexes, and it is quite probable (vide infra) that the contributions of the various mechanisms are different outside this concentration span.

b. Interchange Processes. When CD_2Cl_2 solutions of the complexes [Ni(*R*,*R*:*S*,*S*-tetars)X]ClO_4, X = Cl, Br, or I, are cooled, each shows a similar type of behavior for its 100-MHz NMR spectrum. The sharp two-line methyl proton signals observed at 30° for the chloro complex begin to broaden, the

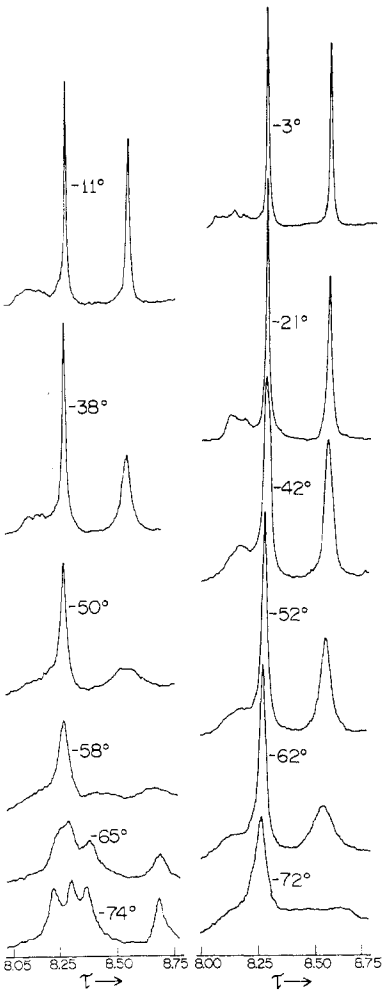

Figure 9. Methyl proton NMR temperature-dependent profiles of (racemic) [Ni(*R*,*R*:*S*,*S*-tetars)Br]ClO_4 (0.04 *M*) on the left and (optically active) [Ni(*R*,*R*-tetars)Br]ClO_4 (0.04 *M*) on the right. The solvent was CD_2Cl_2.

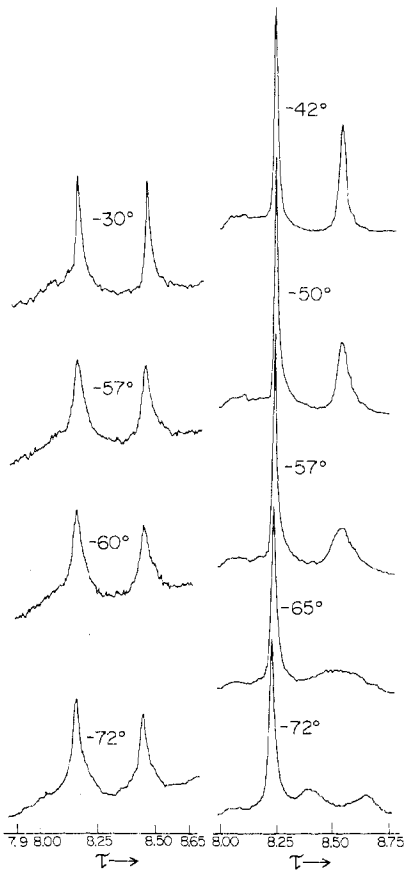

Figure 10. Methyl proton NMR temperature-dependent profiles of [Ni(*R*,*R*:*S*,*S*-tetars)I]I (0.02 *M*) on the left and of [Ni(*R*,*R*:*S*,*S*-tetars)I]ClO_4 (0.04 *M*) on the right; both are in CD_2Cl_2.

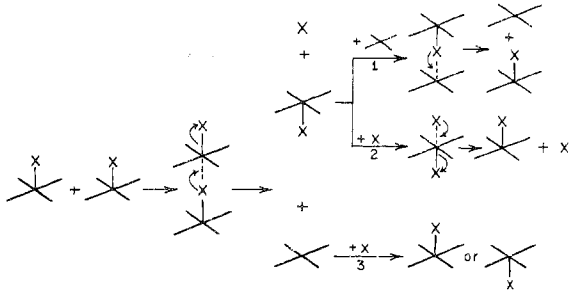

Figure 11. Proposed mechanisms which lead to axial site interchange and intermolecular exchange. The charges associated with the various species are not shown.

higher field signal collapses first, and then, at −72°, a fairly sharp three-line spectrum is observed with the central peak having twice the intensity of the outer two. A similar pattern is observed down to −72° for the bromo species, except that the expected four-line spectrum is resolved due to the slightly different chemical shifts (Figure 9). The spectrum of the iodo complex, however, is not fully collapsed at −72° although the upfield resonance splits into two peaks at this temperature (Figure 10). (Our instrument did not allow us to go to lower temperatures.) In each case, the coalescence temperature of the upfield peak is concentration dependent; the exchange process speeds up as the concentration is increased from 0.01 to 0.04 *M*. When the temperature-dependent spectra of the [Ni(*R*,*R*:*S*,*S*-tetars)Br]ClO_4 and (the optically active) [Ni(*R*,*R*-tetars)Br]ClO_4 species are compared for the same concentration, it is clear that the exchange process for the latter proceeds faster than for the former (Figure 9). Similarly, the temperature-dependent spectra of the complexes [Ni(*R*,*R*:*S*,*S*-tetars)I]ClO_4 and [Ni(*R*,*R*:*S*,*S*-tetars)I]I indicate that the exchange process for the latter is faster than for the former (Figure 10). The chemical shifts for the two iodo species are the same. When, however, the (meso) [Ni(*R*,*S*-tetars)X]ClO_4, X = Cl, Br, or I, complexes dissolved in CD_2Cl_2 are cooled, all three spectra remain essentially unchanged down to −72°. We interpret these results as follows.

It is clear that cooling the [Ni(*R*,*R*:*S*,*S*-tetars)X]ClO_4 complexes slows down the axial-site exchange process to a stage where, at −72°, for the Cl^- and Br^- complexes, the nuclear relaxations are faster than the site exchange. We believe, although these results do not establish, that the [Ni(*R*,*S*-tetars)X]ClO_4 complexes also undergo axial-site exchange but, because the two axial positions are environmentally different, the equilibrium almost exclusively favors one of the sites, probably the one away from the phenyl groups. More will be said about this presently. The observation that the site-exchange velocities for the [Ni(*R*,*R*:*S*,*S*-tetars)X]ClO_4 systems are concentration dependent admits a number of possible mechanisms, but the fact that the optically active species exchange their sites faster than the racemic mixtures provides compelling support to the operation of an associative mechanism, at least as part of the site-exchange process. In Figure 11 we show a possible dimer intermediate consistent with an associative mechanism. On rearrangement, this intermediate will set free a four-coordinate complex, an X^- group, and a site-exchanged five-coordinate complex. The possible fates

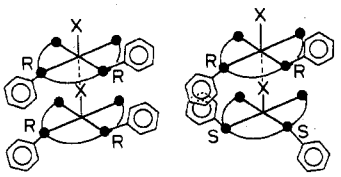

Figure 12. The two dimer intermediates showing the phenyl group interactions. The one on the left is the optically active dimer: the one on the right is the meso dimer. It, of course, is recognized that more than just phenyl group interactions are involved and that the dimer could rotate into a more sterically favorable configuration. But, whatever the configuration, static or fluxional, the two isomers will, in principle, be of different energies.

of these species are shown in the diagram and these, too, can contribute to the site-exchange process by a quasichain mechanism. The subsequent steps shown as 1, 2, and 3 in Figure 11 are almost certainly faster than the formation of the intermediate. The evidence for this is as follows.

We have determined that the visible absorption spectra of the [Ni(*R*,*R*:*S*,*S*-tetars)X]ClO_4 complexes obey Beer's law exactly over the concentration range 10^{-2}–10^{-4} *M* in CH_2Cl_2. This establishes that the standing concentration of the four-coordinate species [Ni(*R*,*R*:*S*,*S*-tetars)]$^{2+}$ is negligible in this concentration range and implies that the velocity of any process which produces the four-coordinate intermediate is much slower than the velocity of the five-coordinate complex formation. Hence it is probable that step 3 is a much more rapid step than the dimer intermediate formation, the destruction of which gives the four-coordinate species. In fact, the addition of X^- to the four-coordinate complex is probably controlled to a large extent by diffusion in CH_2Cl_2. We know that step 2 is fast because the site-exchange process for the [Ni(*R*,*R*:*S*,*S*-tetars)I]I complex is faster than for the [Ni(*R*,*R*:*S*,*S*-tetars)I]ClO_4 species (Figure 10) and we think this is because, in the former, the associative mechanism is bypassed and the mechanism in step 2 predominates. Similarly, catalysis occurs by the addition of ClO_4^- ions. Thus a CD_2Cl_2 solution of tetraphenylarsonium perchlorate (0.01 *M*) and [Ni(*R*,*R*:*S*,*S*-tetars)Br]ClO_4 (0.04 *M*) gives the same temperature-dependent spectra as shown in Figure 9, except that each of the events occurs at about 10° lower in temperature. This implies that, although site exchange occurs via the dimer intermediate, some of the exchange also occurs through ClO_4^- reaction as depicted in step 2. Similar, but much more pronounced catalysis, is observed when Br^- ions are added to the [Ni(*R*,*R*:*S*,*S*-tetars)Br]ClO_4 complex. We have established that step 1 is also a fast process. When the complex [Ni(*R*,*R*:*S*,*S*-tetars)]$(ClO_4)_2$ (0.004 *M*) is added to a 0.04 *M* CD_2Cl_2 solution of [Ni(*R*,*R*:*S*,*S*-tetars)Br]ClO_4, the successive events in the NMR temperature profile are identical with those shown in Figure 9 except that each event occurs about 20° lower in temperature.[15] Thus, the presence of a catalytic amount of [Ni(*R*,*R*:*S*,*S*-tetars)]$(ClO_4)_2$ speeds up the interchange process, which suggests that step 1 is a faster process than the dimer intermediate formation.

For the racemic mixture, the dimer intermediate can exist as two energetically distinct diastereomeric pairs, either [(*R*,*R*-tetars)Ni–X---Ni(*R*,*R*-tetars)X]$^{2+}$ or [(*R*,*R*-tetars)-Ni–X---Ni(*S*,*S*-tetars)X]$^{2+}$ or the respective enantiomorphs which, of course, are of identical energy. The optically active complex can form only one of these, the first or its enantiomorph. Other chemical evidence derived from dimers formed with these ligands[16] suggests that the optically active, rather than the meso, dimer is the more stable. This is consistent with the observations here, where the exchange through dimer formation is faster for the optically active complexes. Figure 12 shows the two dimers diagramatically and emphasizes the different phenyl group interactions in the two cases which, molecular models suggest, would be greater for the meso dimer.

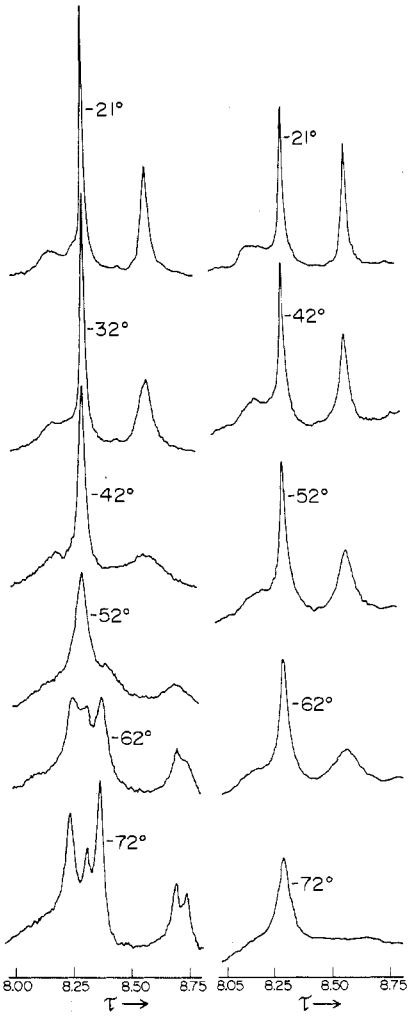

Figure 13. Methyl proton NMR temperature-dependent profiles of a mixture of the [Ni(*R*,*R*:*S*,*S*-tetars)Cl]ClO_4 (0.02 *M*) and [Ni(*R*,*R*:*S*,*S*-tetars)Br]ClO_4 (0.02 *M*) (racemic) complexes on the left and profiles for the (optically active) mixture of [Ni(*R*,*R*-tetars)Cl]ClO_4 (0.02 *M*) and [Ni(*R*,*R*-tetars)Br]ClO_4 (0.02 *M*) on the right. Both are in CD_2Cl_2.

c. Exchange Processes. The exchange processes show remarkably similar NMR patterns to those observed for the axial-site interchange phenomena. Figure 13 shows the CD_2Cl_2 solution temperature-dependent NMR profiles of the mixture [Ni(*R*,*R*:*S*,*S*-tetars)Br]ClO_4 (0.02 *M*) and [Ni(*R*,*R*:*S*,*S*-tetars)Cl]ClO_4 (0.02 *M*) as well as those for the optically active mixture [Ni(*R*,*R*-tetars)Br]ClO_4 (0.02 *M*) and [Ni(*R*,*R*-tetars)Cl]ClO_4 (0.02 *M*).[17] Similar behavior was observed for the chloro–iodo and bromo–iodo mixtures. In all cases, the exchange process becomes faster as the concentration is increased. Moreover, as was observed for the case of the interchange reactions, the profiles in Figure 13 clearly show that the exchange process for the optically active complexes is faster than when the same process involves a racemic mixture at the same concentration. This fact, together with the concentration dependence of the rate, strongly suggests that the exchange reactions also involve formation of a dimer intermediate of the kind depicted in Figure 12 as an important constituent of the mechanism. We were unable satisfactorily to repeat the experiments involving the addition of halide and perchlorate ions described for the interchange reactions because of solubility problems, although there was a speed-up of exchange when a catalytic amount (~5%) of

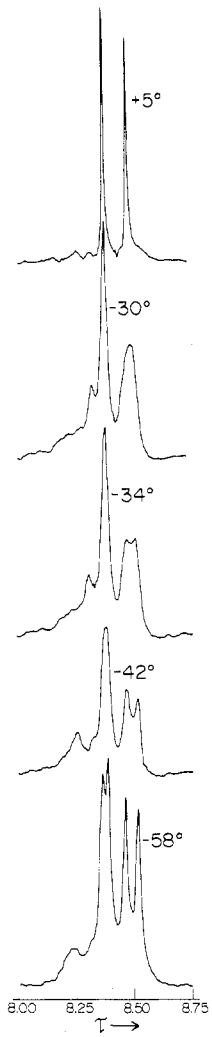

Figure 14. Methyl proton NMR temperature-dependent profiles of a mixture of the [Ni(*R*,*S*-tetars)Cl]ClO_4 (0.02 *M*) and [Ni(*R*,*S*-tetars)Br]ClO_4 (0.02 *M*) (meso) complexes dissolved in CD_2Cl_2.

[Ni(*R*,*R*:*S*,*S*-tetars)]$(ClO_4)_2$ was added to the chloro–bromo mixture.

It is interesting, however, that the [Ni(*R*,*R*:*S*,*S*-tetars)Cl]ClO_4 and the [Ni(*R*,*R*:*S*,*S*-tetars)Br]ClO_4 complexes, which have similar chemical shifts for their methyl proton resonances,[17] are observed to have similar (interchange) coalescence temperatures which, in turn, are similar to those observed for the chloro–bromo (exchange) mixtures at the same total complex concentration (cf. Figures 9 and 13). This observation, together with the fact that the exchange and interchange reactions respond in a similar way to the imposed kinetic constraints, suggests that the mechanisms for the two processes are the same and proceed at similar rates. Thus we conclude, mutatis mutandis, that the mechanisms and intermediates shown in Figures 11 and 12 also apply to the exchange reactions. To some extent this conclusion logically follows once the presence of a dimer intermediate is established for both processes, for an associative exchange process at one and the same time involves axial-site exchange.

We have not investigated the exchange reactions of the meso ligand complexes in the same detail as those just described for the racemic analogue. Figure 14 shows the CD_2Cl_2 temperature-dependent NMR profile for the (equal) mixture of [Ni(*R*,*S*-tetars)Cl]ClO_4 and [Ni(*R*,*S*-tetars)Br]ClO_4. It will be seen that the spectra eventually collapse into the expected four resonances at −58°; the chemical shifts correspond exactly to those observed for the isolated complexes at this temperature. As for the racemic analogue, the exchange rate is concentration dependent, and the reactions go faster as the concentration is increased. This suggests, but does not prove, that an associative mechanism also operates for the meso ligand exchange reactions. If this is so and the intermediate is similar to that shown in Figure 12, then axial-site exchange occurs with these complexes. This, however, can only be reconciled with the fact that it appears that only one axial isomer exists in appreciable standing concentrations (the +30 and −72° spectra for the isolated complexes are the same) if it is assumed there is a rapid kinetic path, which converts the associatively formed unstable isomer to the stable axial geometry.

We have obtained some evidence to support this hypothesis that the thermodynamically unstable axial site is important in the kinetic exchange process. Thus, when the solution mixture of [Ni(*R*,*S*-tetars)Cl]ClO_4 (0.02 *M*), [Ni(*R*,*S*-tetars)Br]ClO_4 (0.02 *M*), Ph_4AsCl (0.004 *M*), and Ph_4AsBr (0.004 *M*) in CD_2Cl_2 is cooled, only two lines are observed at −72°. The two methyl proton lines are only slightly broader at −72° than they are at 30°. This is a similar catalysis to that observed for the racemic analogues and suggests that the free halide ions engage in bimolecular displacement reactions involving the unstable axial site (cf. step 2, Figure 11).

d. Palladium Complexes. Finally, all of the five-coordinate palladium and platinum complexes of these ligands show only two sharp methyl proton signals at 30° in all solvents investigated, suggesting that these too are undergoing rapid axial-site exchange. Most of these are much less soluble in acceptable solvents than the nickel analogues and we were unable properly to investigate the kinetics. The most soluble of these, [Pd(*R*,*R*:*S*,*S*-tetars)Cl]ClO_4, has similar 30° chemical shifts for the methyl proton resonances in CD_2Cl_2 as those of the nickel analogue (for Ni, τ 8.35, 8.61; for Pd, τ 8.18, 8.56), but at −72°, the two signals only became about 4 times broader at half-height, and there is no coalescence or collapse of the lines, as is observed for the nickel complexes. This suggests that the palladium interchange reactions are faster than those of nickel. Assuming the same mechanism for the palladium interchange, this observation is interesting to the extent that substitution within four-coordinated complexes is generally faster for divalent nickel than for palladium. We, however, prefer not to speculate a posteriori on the apparent reversal in rates of substitution for these five-coordinate complexes.

Acknowledgment. We thank the NRC and the Chemistry Department of the University of Toronto for financial support.

Registry No. [Ni(*R*,*R*:*S*,*S*-tetars)]$(ClO_4)_2$, 56727-99-2; [Ni(*R*,*R*-tetars)]$(ClO_4)_2$, 56781-76-1; [Ni(*R*,*S*-tetars)]$(ClO_4)_2$, 56781-78-3; [Ni(*R*,*R*;*S*,*S*-tetars)CH_3CN]$(ClO_4)_2$, 56781-61-4; [Ni(*R*,*R*-tetars)CH_3CN]$(ClO_4)_2$, 56727-90-3; [Ni(*R*,*S*-tetars)-CH_3CN]$(ClO_4)_2$, 56781-74-9; [Ni(*R*,*R*:*S*,*S*-tetars)Cl]ClO_4, 56781-72-7; [Ni(*R*,*R*-tetars)Cl]ClO_4, 56781-70-5; [Ni(*R*,*S*-tetars)Cl]ClO_4, 56727-97-0; [Ni(*R*,*R*:*S*,*S*-tetars)Br]ClO_4, 56781-68-1; [Ni(*R*,*R*-tetars)Br]ClO_4, 56727-92-5; [Ni(*R*,*S*-tetars)Br]ClO_4, 56781-63-6; [Ni(*R*,*R*:*S*,*S*-tetars)I]ClO_4, 56727-94-7; [Ni(*R*,*R*:*S*,-*S*-tetars)I]I, 56727-95-8; [Ni(*R*,*R*-tetars)I]I, 56781-64-7; [Ni(*R*,-*S*-tetars)I]ClO_4, 56781-66-9; [Pd(*R*,*R*:*S*,*S*-tetars)Cl]Cl, 56781-79-4; [Pd(*R*,*R*-tetars)Cl]Cl, 56727-81-2; [Pd(*R*,*S*-tetars)Cl]Cl, 56781-42-1; [Pd(*R*,*R*:*S*,*S*-tetars)]$(ClO_4)_2$, 56727-83-4; [Pd(*R*,*R*-tetars)]$(ClO_4)_2$, 56781-48-7; [Pd(*R*,*S*-tetars)]$(ClO_4)_2$, 56781-50-1; [Pd(*R*,*R*:*S*,*S*-tetars)Cl]ClO_4, 56781-44-3; [Pd(*R*,*S*-tetars)Cl]ClO_4, 56781-46-5; [Pd(*R*,*R*:*S*,*S*-tetars)Br]ClO_4, 56727-85-6; [Pd(*R*,*R*-tetars)Br]Br, 56781-51-2; [Pd(*R*,*S*-tetars)Br]ClO_4, 56781-53-4; [Pd(*R*,*R*-tetars)I]I, 56727-80-1; [Pd(*R*,*S*-tetars)I]I, 56781-41-0; [Pt(*R*,*R*:*S*,*S*-tetars)]-$(ClO_4)_2$, 56727-87-8; [Pt(*R*,*R*-tetars)]$(ClO_4)_2$, 56781-55-6; [Pt-(*R*,*S*-tetars)]$(ClO_4)_2$, 56781-57-8; [Pt(*R*,*R*:*S*,*S*-tetars)I]I, 56727-88-9; [Pt(*R*,*R*-tetars)I]I, 56781-58-9; [Pt(*R*,*S*-tetars)I]I, 56781-59-0; [Ni$(H_2O)_6$]$(ClO_4)_2$, 10171-10-5; [Pd$(CH_3CN)_2Cl_2$], 14592-56-4.

Supplementary Material Available. The whole of the Experimental Section of this paper will appear following these pages in the microfilm edition of this volume of the journal. The Experimental Section contains a description of the instrumentation and the details of the preparation and isolation of all of the compounds listed in Tables I–III, as well as the optically active species. In addition, the Experimental Section contains a description of the morphologies of the crystals, the optical rotations, and the analytical data. Photocopies of the supplementary material from this paper only or microfiche (105 × 148 mm, 24× reduction, negatives) containing all of the supplementary material for the papers in this issue may be obtained from the Business Office, Books and Journals Division, American Chemical Society, 1155 16th St., N.W., Washington, D.C. 20036. Remit check or money order for $4.50 for photocopy or $2.50 for microfiche, referring to code number AIC50271C-12-75.

References and Notes

(1) R. S. Nyholm, *J. Chem. Soc.*, 2061 (1950).
(2) C. M. Harris, R. S. Nyholm, and F. J. Phillips, *J. Chem. Soc.*, 4379 (1960).
(3) C. M. Harris and R. S. Nyholm, *J. Chem. Soc.*, 4375 (1956).
(4) L. M. Venanzi, *Angew. Chem., Int. Ed. Engl.*, **3**, 453 (1964).
(5) J. W. Dawson and L. M. Venanzi, *J. Am. Chem. Soc.*, **90**, 7229 (1968).
(6) G. S. Benner and D. W. Meek, *Inorg. Chem.*, **6**, 1399 (1967).
(7) B. Bosnich, W. G. Jackson, and S. B. Wild, *J. Am. Chem. Soc.*, **95**, 8269 (1973).
(8) B. Bosnich, W. G. Jackson, and S. B. Wild, *Inorg. Chem.*, **13**, 1121 (1974).
(9) J. R. Preer and H. B. Gray, *J. Am. Chem. Soc.*, **92**, 7306 (1970).
(10) R. Ettore, G. Dolcetti, and A. Peloso, *Gazz. Chim. Ital.*, **97**, 1681 (1967).
(11) W. J. Geary, *Coord. Chem. Rev.*, **7**, 81 (1971).
(12) B. Bosnich, W. G. Jackson, and S. T. D. Lo, *Inorg. Chem.*, **14**, 1460 (1975).
(13) W. Moffitt, *J. Chem. Phys.*, **25**, 1189 (1956).
(14) G. Dyer, J. G. Hartley, and L. M. Venanzi, *J. Chem. Soc.*, 1293 (1965).
(15) It should be noted that the total ClO_4^- concentration in this experiment is less than that of the (0.01 *M*) perchlorate catalysis experiment and that the signal amplitude was such that the NMR spectrum of the [Ni(*R*,*R*:*S*,*S*-tetars)]$(ClO_4)_2$ was barely detectable.
(16) B. Bosnich, W. G. Jackson, and S. T. D. Lo, *Inorg. Chem.*, **13**, 2598 (1974).
(17) The chemical shifts of the methyl proton peaks at −72° correspond exactly to those observed for the interchange experiments. Thus for [Ni(*R*,*R*:*S*,*S*-tetars)Cl]ClO_4, the collapsed methyl proton resonances occur at, τ 8.24, 8.36, (twice the intensity), and 8.75; for [Ni(*R*,*R*:*S*,*S*-tetars)Br]ClO_4, these occur at τ 8.22, 8.30, 8.36, and 8.68; and for the equal mixture, these occur at τ 8.23 (twice the intensity), 8.30, 8.36 (twice the intensity), 8.68, and 8.75 (Figure 13).

Contribution from the Departments of Chemistry, University of North Carolina, Chapel Hill, North Carolina 27514, and Grinnell College, Grinnell, Iowa 50112

Carbon-13 Nuclear Magnetic Resonance Studies of Platinum(II) Complexes. I. Five-Membered Rings Formed by Substituted 1,2-Diaminoethanes

LUTHER E. ERICKSON,[1a] JOSEPH E. SARNESKI,[1b] and CHARLES N. REILLEY*[1b]

Received April 23, 1975 AIC50279M

The ^{13}C NMR spectra of a series of aqueous square-planar platinum(II) chelates, Pt(bpy)(substituted 1,2-diaminoethane)$^{2+}$, have been obtained for 13 different diamines. ^{13}C chemical shifts of the bipyridine carbons are fairly constant across this entire series; in chelates of nonsymmetric diamines nonequivalent resonances are found for the two bipyridyl rings. ^{13}C resonances of the aliphatic diamine portion resemble those of the free ligand with carbons α to the nitrogen donors showing a 2–10-ppm downfield shift due to platinum binding. Platinum–carbon spin coupling interactions are generally seen for the diamine carbons. $^2J_{PtC}$ for *N*-methyl carbons varies from 10 to 25 Hz, decreasing for *N*,*N*-dimethyl substitution. $^3J_{PtC}$ values of 20–50 Hz were observed; these data and the known conformational properties of gauche five-membered diamine rings suggest a Karplus-like dependence for $^3J_{PtC}$. Using this $^3J_{PtC}$ information and complementary $^3J_{HH}$, $^3J_{PtH}$, and $^4J_{PtH}$ data an analysis of the conformational properties of gauche 1,2-diamine chelate rings of 1,2-diaminopropane (pn) and its two *N*,*N*-dimethyl-substituted analogs (*N*,*N*-Me2pn) was made. Substantial preference for *C*-methyl equatorial orientation is indicated for pn and N^1,N^1-Me2pn complexes; N^2,N^2-Me2pn has nearly equal distribution of axial and equatorial *C*-methyl conformers. Coupling of platinum to the carbon nuclei forming the five-membered rings is highly structurally dependent, being near zero in symmetric rings but 10–15 Hz in unsymmetrical diamine chelates. These observations are explained via a multipath coupling mechanism. Model compounds designed to exclude multipath coupling mechanisms support this type of analysis. ^1H spectra measured at various frequencies from 30 to 300 MHz illustrate a pronounced broadening of platinum satellites at higher fields; at 300 MHz platinum satellites are broadened beyond recognition.

Introduction

Ever since Karplus' classic 1959 paper on the dihedral angle dependence of the three-bond vicinal coupling constant, $^3J_{H-H}$, in H–C–C–H fragments,[2] chemists have attempted to establish molecular geometries from NMR coupling constants. Considerable success has been achieved in extending the Karplus model to analyze empirically variation in coupling constants with dihedral angle in other four-atom fragments.[3] In particular, the dihedral angle dependence of $^3J_{Pt-H}$ in Pt–N–C–H fragments in amino acid chelates was shown to parallel reasonably closely the Karplus curve for $^3J_{H-H}$.[4] More extensive studies of diamine and amino acid complexes of platinum confirmed the earlier suggestions and also established a parallel dependence of $^4J_{Pt-H}$, in Pt–N–C–CH_3 fragments, on the dihedral angle between the Pt–N and the C–C bonds.[5,6] $^4J_{PtH}$ appears to be relatively large (~7 Hz) for $\phi = 180°$ and to drop off rapidly with decreasing angle.

With the availability of spectrometers capable of obtaining ^{13}C NMR spectra of natural-abundance samples, parallel studies to establish the dihedral angle dependence of $^3J_{Pt-C}$ for coupling between ^{13}C ($I = 1/2$, 1% abundance) and ^{195}Pt ($I = 1/2$, 33% abundance) have become feasible. In proton-decoupled carbon-13 spectra, $^3J_{C-Pt}$ can be determined readily as the spacing between the doublet satellites which surround the singlet signal from each different carbon. Thus, if a relatively simple relation between $^3J_{Pt-C}$ and dihedral angle could be established, conformational information for platinum chelates could be obtained readily from ^{13}C spectra as is suggested by a recent ^{13}C study of platinum chelates of *meso*- and *rac*-2,3-diaminobutanes.[7] In view of the difficulty encountered in trying to decipher platinum–proton coupling superimposed on already complex proton-coupled multiplets present in many chelates, ^{13}C–^{195}Pt coupling could offer a much more straightforward approach to conformational studies of platinum complexes.

In addition to this simplifying feature, coupling of platinum